AMORPHOUS AND NANOCRYSTALLINE SOFT MAGNETS

G .Herzer
Vacuumschmelze GmbH & Co KG

Manuscript published in:

Proceedings of the NATO Advanced Study Insititute on
Magnetic Hysteresis in Novel Materials,
Mykonos, Greece, 1-12 July 1996

ed. George C. Hadjipanayis

Nato ASI Series (Series E:Applied Sciences Vol. 338)
Kluwer Academic Publishers (Dordrecht/Boston/London) 1997

(ISBN 0-7923-4604-1)

AMORPHOUS AND NANOCRYSTALLINE SOFT MAGNETS

GISELHER HERZER
Vacuumschmelze GmbH
D-63450 Hanau, Germany

Abstract **–** The article surveys amorphous and nanocrystalline alloys for soft magnetic applications. Both materials have much in common starting from their way of production and ranging over to the key factors which determine their properties. Thus, the magneto-crystalline anisotropy is randomly fluctuating on a scale much smaller than the domain wall width and, as a consequence, is averaged out by exchange interaction so that there is no anisotropy net effect on the magnetization process – the prerequisite for good soft magnetic behavior. Superior soft magnetic properties additionally require a low magnetostriction which is realized for amorphous Co-based alloys and, more recently, for nanocrystalline Fe-base alloys but at a significantly higher saturation induction and better thermal stability. Both materials reveal low losses up to several 100 kHz and their B-H loop can be tailored by magnetic field annealing according to the demands of application.

1 Introduction

Amorphous metals for soft magnetic applications are produced by rapid solidification from the melt (cf. [1]) as thin ribbons typically around 20 µm thick and from about 1 mm to 100 mm wide. Typical compositions are $(Fe,Co,Ni)_{70\text{-}85}(Si,B)_{15\text{-}30}$ at% (cf. [2]) whereby the metalloids Si and B are necessary for glass formation and in order to stabilize the amorphous structure. The detailed composition can be widely varied which allows to cover a large spectrum of soft magnetic properties according to the demands of numerous applications. Since their discovery, about three decades ago, the crystallization of amorphous metals was known to deteriorate their soft magnetic properties significantly and to yield a relatively coarse microstructure with grain sizes of about 0.1-1 µm. In 1988, however, it was found [3] that the crystallization of Fe-(Si,B) glasses with the combined addition of small amounts of Cu and Nb yields an ultrafine grain structure of bcc-FeSi with grain sizes of typically 10-15 nm embedded in an amorphous minority matrix. These new *nanocrystalline* alloys moreover revealed superior soft magnetic properties so far only achieved by permalloys and Co-based amorphous alloys, but at a significantly higher saturation induction of 1.2 Tesla and even more. Table 1 summarizes the typical soft magnetic properties of amorphous and nanocrystalline alloys together with the properties of conventional highly permeable materials.

It is well known that the microstructure, noticeably the structural correlation length, essentially determines the hysteresis loop of a ferromagnetic material. Figure 1 summarizes our present understanding of the coercivity, H_c, in the whole range of structural correlation lengths starting from atomic distances in amorphous alloys over grain sizes, D, in the nanometer regime up to macroscopic grain sizes – the

TABLE 1. Typical values of grain size D, saturation magnetization J_s, saturation magnetostriction λ_s, coercivity H_c, initial permeability μ_i, electrical resistivity ρ, core losses P_{Fe} at 0.2 T, 100 kHz and ribbon thickness t for nanocrystalline, amorphous and crystalline soft magnetic ribbons.

Alloy	D (nm)	J_s (T)	λ_s (10^{-6})	H_c (A/m)	μ_i (1 kHz)	ρ (μΩcm)	P_{Fe}(W/kg)	t (μm)	Ref.
$Fe_{73.5}Cu_1Nb_3Si_{13.5}B_9$	13	1.24	2.1	0.5	100 000	118	38	18	(a)
$Fe_{73.5}Cu_1Nb_3Si_{15.5}B_7$	14	1.23	~0	0.4	110 000	115	35	21	(b)
$Fe_{84}Nb_7B_9$	9	1.49	0.1	8	22 000	58	76	22	(c)
$Fe_{86}Cu_1Zr_7B_6$	10	1.52	~0	3.2	48 000	56	116	20	(c)
$Fe_{91}Zr_7B_3$	17	1.63	-1.1	5.6	22 000	44	80	18	(c)
$Co_{68}Fe_4(MoSiB)_{28}$	amorphous	0.55	~0	0.3	150 000	135	35	23	(b)
$Co_{72}(FeMn)_5(MoSiB)_{23}$	amorphous	0.8	~0	0.5	3 000	130	40	23	(b)
$Fe_{76}(SiB)_{24}$	amorphous	1.45	32	3	8 000	135	50	23	(b)
80%Ni-Fe (permalloys)	~100 000	0.75	<1	0.5	100 000 (d)	55	>90 (e)	50	(b)
50%-60%Ni-Fe	~100 000	1.55	25	5	40 000 (d)	45	>200 (e)	70	(b)

(a) after ref. [3]
(b) typical commercial grades for low remanence hysteresis loops [10, 11]
(c) after ref. [12]
(d) 50 Hz- values
(e) lower bounds due to eddy currents

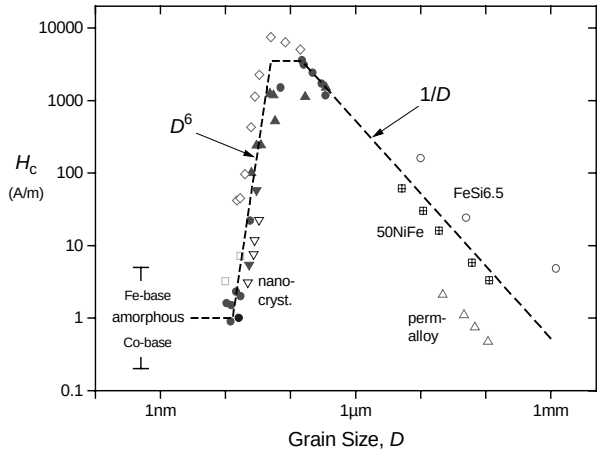

Figure 1. Coercivity, H_c, vs. grain size, D, for various soft magnetic metallic alloys (after [8,9]): Fe-$Nb_3Si_{13.5}B_9$ (solid up triangles), Fe-$Cu_1Nb_{1\text{-}3}Si_{\sim 13}B_{\sim 9}$ (solid circles), Fe-$Cu_1V_{3\text{-}6}Si_{12.5}B_8$ (solid down triangles), Fe-$Cu_1V_xSi_{19\text{-}x}B_8$ (open down triangles), Fe-$Cu_{0\text{-}1}Zr_{\sim 7}B_{2\text{-}6}$ (open squares), $Fe_{60}Co_{30}Zr_{10}$ (open diamonds), NiFe-alloys (+ center squares and open up triangles) and FeSi6.5wt% (open circles).

permeability shows an analogous behavior being essentially inversely proportional to H_c. The 1/D-dependence of coercivity for large grain sizes (cf. [4]) reflects the conventional rule that good soft magnetic properties require very large grains (D > 100 µm). Thus, the reduction of particle size to the regime of the domain wall width increases the coercivity H_c towards a maximum controlled by the anisotropies present. Accordingly, fine particle systems have been mostly discussed as hard magnetic materials (cf. [5]). Lowest coercivities, however, are again found for smallest structural correlation lengths like in amorphous alloys ("grain size" of the order of atomic distances) and in nanocrystalline alloys for grain sizes D < 20 nm. Obviously, the new nanocrystalline material fills in the gap between amorphous metals and conventional poly-crystalline alloys. The extraordinary D^6-dependence of coercivity at small grain size moreover demonstrates how closely soft and hard magnetic behavior actually can be neighbored. Indeed, the soft magnetic alloys are only one manifestation of the novel and extraordinary magnetic properties which can be realized by establishing structural features on the nanometer scale. Thus, nanocrystalline microstructures are also of highly current interest in order to enhance the properties of rare earth hard magnets (cf. [6]).

The decrease of coercivity in the new nanocrystalline materials has to be well distinguished from superparamagnetic phenomena i.e. the well-known decrease of coercivity in small, isolated or weakly coupled particles due to thermal excitation (cf. [5]). Although coercivity vanishes, the superparamagnetic regime is not very interesting for soft magnetic application since an appreciable change of magnetization requires large magnetic fields, i.e. the permeability is fairly low. In the present case we deal with small ferromagnetic crystallites well coupled by exchange interaction and with low coercivity and simultaneously high permeability [7,8].

2 Basic Concepts

The combination of small grain size and soft magnetic properties is surprising and fascinating from the classical point of view in magnetic engineering. Yet, this possibility was principally known from amorphous materials and the theoretical interpretation of their soft magnetic properties. Accordingly, magnetic softening should also occur as soon as the structural correlation length or grain size becomes smaller than the ferromagnetic exchange length which is in the order of the domain wall width. In this case the local anisotropies are randomly averaged out by exchange interaction so that there is no anisotropy net effect on the magnetization process. The degree to which the local anisotropies are finally averaged out can be addressed in terms of the so-called *random anisotropy model* . The model has been originally developed by Alben et al. [13] for amorphous metals and, later on, could be successfully applied to explain the behavior of the nanocrystalline materials [7, 8]. Accordingly, the average magneto-crystalline anisotropy, $\langle K \rangle$, scales with the structural correlation length, D, like

$$\langle K \rangle \sim K_1 \, (D/L_0)^6 \tag{1}$$

where $L_0=(A/K_1)^{½}$ is the basic ferromagnetic correlation length determined by the local anisotropy constant K_1 and the exchange stiffness A. Table 2 summarizes the results for the relevant material parameters in 3d- and 4f- amorphous metals (cf. [14]) as well as for a typical nanocrystalline alloy. Thus, the magneto-crystalline anisotropy is reduced by orders of magnitude towards a few J/m^3, i.e. small enough to enable good soft magnetic behavior except for 4f- amorphous metals like $Tb_{33}Fe_{67}$ (cf. [13]) with strong local anisotropies.

TABLE 2. Typical values for the structural correlation length D, the local anisotropy constant K_1, the basic ferromagnetic correlation length L_0, and the effective, averaged anisotropy $\langle K \rangle$ for amorphous 3d- and 4f-metals and for nanocrystalline bcc-$Fe_{80}Si_{20}$, the constituent phase in $Fe_{73.5}Cu_1Nb_3Si_{13.5}B_9$. A value of $A \approx 10^{-11}$ J/m has been assumed for the exchange stiffness in all cases.

	amorphous 3d metals		nanocrystalline $Fe_{80}Si_{20}$	amorphous 4-f metals	
D (nm)	0.5		10	0.5	
K_1 (J/m^3)	10^4	10^5	8×10^3	10^6	10^7
L_0 (nm)	30	10	35	3	1
$\langle K \rangle$ (J/m^3)	2.1×10^{-7}	1.6×10^{-3}	4	21	1.5×10^5

Actually, the understanding of magnetic anisotropies and how they can be controlled is the key factor in order to tailor the engineering properties of any ferromagnet. Thus, the coercivity, H_c, and the initial permeability, μ_i, can be related to the anisotropy constant K by

$$H_c \approx 2K / J_s \,, \quad \mu_0 \, \mu_i \approx J_s^2 / 2K \,. \tag{2}$$

Although only strictly valid for coherent domain rotation, these relations in most cases allow at least a rough estimate of the order of H_c and μ_i . Accordingly, the basic conditions for good soft magnetic properties generally are low or vanishing magnetic anisotropies of a few J/m^3 only. The angular distribution of the anisotropy axis finally controls the shape of the hysteresis loop.

The relevant anisotropy contributions are in decreasing order of magnitude:

1. the magneto-crystalline anisotropy,
2. magneto-elastic anisotropies and
3. uniaxial anisotropies induced by annealing.

The prerequisite for good soft magnetic behavior is that the effective magneto-crystalline anisotropy is low, which in both amorphous and nanocrystalline materials is realized by the averaging effect of exchange interaction.

Superior properties, however, additionally require a low or vanishing magnetostriction, λ_s, which reduces magneto-elastic anisotropies

$$K_\sigma = -\tfrac{3}{2}\lambda_s\sigma \tag{3}$$

arising from internal or external mechanical stress, σ . Such internal stresses are introduced during the preparation process and by winding the ribbons to toroidal cores (the major form of application) and, in the as prepared state, are typically in the order of $\sigma \approx$ 100 MPa. Thus, optimization of the magnetic properties first of all requires a stress relief treatment by annealing at possibly high temperatures. Still, typically a few percent of these stresses remain even after a good stress relief treatment - additional stresses may occur from handling and housing the toroids. The associated magneto-elastic anisotropies, of course, put limits to the achievable soft magnetic properties. Thus, in highly magnetostrictive Fe-base alloys ($\lambda_s \approx 30$ ppm), the initial permeability is typically limited to $\mu_i \approx 10\,000$ even after stress relief treatment. Accordingly, highest initial permeabilities of 100 000 or more can only be achieved by reducing the magnetostriction considerably.

Once magneto-crystalline anisotropy and magnetostriction are sufficiently suppressed, the magnetic properties are determined by uniaxial anisotropies induced during the heat treatment either by a magnetic field or by mechanical creep. In particular the magnetic field induced anisotropies are of huge practical relevance and, if properly controlled, allow to tailor the hysteresis loop according to the demands of application.

3 Alloy Systems

The range of compositions which can be prepared in the glassy state by rapid solidification from the melt is wide. Typical compositions are given by the formula $T_{70\text{-}90}X_{10\text{-}30}$ (at%). T stands for a practically arbitrary combination of transition metals which for magnetic applications are of course Fe, Co and Ni. X refers to metalloid atoms like Si and B and/or refractory metals like Nb, Mo, Zr, Hf etc. These additions guarantee glass formation and stabilize the amorphous structure since their atomic volume is either considerably smaller or larger than that of the transition metals Fe, Co and Ni.

The most common compositions for soft magnetic applications either in the amorphous or in the nanocrystalline state are metal-metalloid based (Fe, Co, Ni)-(Si,B) alloys with small additions of Mn, Nb, C and, for the nanocrystalline case, of Cu. This alloy system has a good glass forming ability and is easily accessible by rapid solidification as a thin ribbon in large scale production.

A second family of Fe-Zr (B) based alloys have gained particular interest concerning their properties after nanocrystallisation. These alloys and derivatives are currently still under intensive research. Their major draw-back is a lower glass forming ability and/or castability due to the oxygen reactivity of the Zr addition. Thus, these alloys presently are still restricted to the laboratory scale, since they require a by far more sophisticated production technology than the metal-metalloid based compositions.

3.1 AMORPHOUS ALLOYS

The fundamental properties of amorphous alloys are the saturation magnetization J_s , the magnetostriction constant λ_s, the Curie temperature T_c and their crystallization temperature, T_x. Some characteristic examples are summarized in Figs. 2 and 3 which show the influence of the transition metal and the metalloid content, respectively.

The saturation magnetization J_s is the highest in the Fe-rich alloys and decreases with increasing Ni and Co content. It is generally lower than in crystalline alloys due to the non-magnetic additions of Si and B necessary for glass formation. The J_s -maximum observed for crystalline Fe-Co alloys is only weakly developed and shifted to the Fe-rich side.

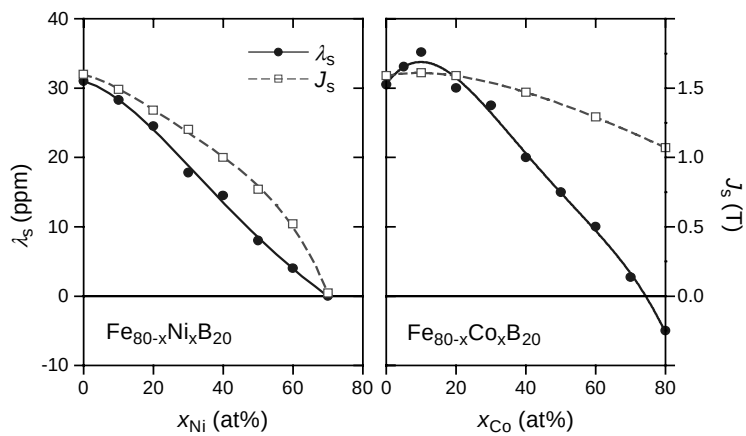

Figure 2. Saturation magnetostriction, λ_s , (full lines) and saturation magnetization, J_s, (dashed lines) in amorphous Fe-Ni- and Fe-Co-base alloys (after ref. [2] and references therein)

The second fundamental magnetic parameter determined by mainly the transition metals is the magnetostriction which is isotropic in the amorphous state. For the Fe-rich alloys the saturation magnetostriction λ_s is positive, typically $\lambda_s \approx 20$ - 40 ppm, while for

the Co-rich alloys, λ_s is negative, typically $\lambda_s \approx$ -5 to - 3 ppm. The decrease of λ_s with increasing Ni-content is correlated to the simultaneous decrease of the saturation magnetization ($|\lambda_s| \propto J_s^2$). Thus, the apparent disappearance of λ_s at high Ni-contents only occurs because the system becomes paramagnetic. A true zero of magnetostriction only occurs on the Co-rich side of Co-Fe [15] or Co-Mn [16] based systems at Fe or Mn concentrations of about 3-8 at%.

Thus, according to their magnetostriction amorphous materials are commonly divided into two major groups: the Fe-based and Co-based alloys. The Fe-based amorphous alloys are based on inexpensive raw materials, have a high saturation magnetization but their magnetostriction is large which limits their soft magnetic behavior. On the other hand, Co-based amorphous alloys with small additions of Fe or Mn reveal nearly zero magnetostriction. Accordingly, they can offer superior soft magnetic behavior, but their saturation magnetization is considerably lower than for the Fe-based materials.

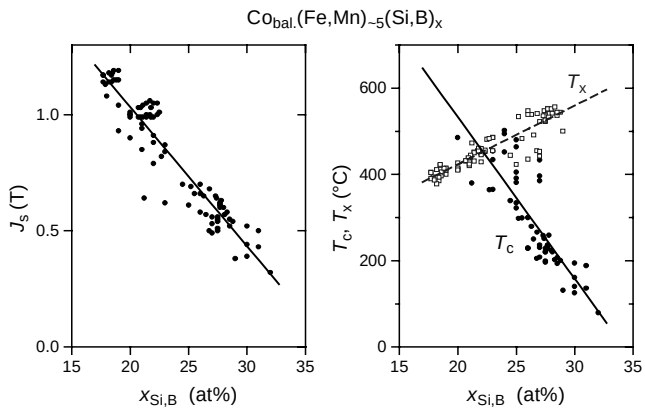

Figure 3. Saturation magnetization, J_s, Curie temperature, T_c, and crystallization temperature, T_x, of near-zero magnetostrictive Co-base alloys vs. the total metalloid contents.

Apart from the metallic components, the magnetic properties are still determined by the metalloid-contents. The effect is minor in Fe-based alloys but very pronounced in Co-based systems. As demonstrated in Figure 3, saturation inductions up to 1.2 T can be achieved in Co-based alloys by reducing the metalloid contents below about 20 at%. However, these high J_s -alloys are close to the boundary of glass formation and reveal a low crystallization temperature, T_x, which at the same time diminishes the thermal stability of the magnetic properties. Furthermore high J_s -alloys reveal a strong field induced anisotropy and correspondingly low permeabilities. Actually, high permeabilities of $\mu_i > 100\,000$ can only be obtained in the high metalloid compositions with $J_s < 0.6$ T and $T_c < 250$°C (cf. table 1).

3.2 NANOCRYSTALLINE ALLOYS

Principally, nanocrystalline alloys can be synthesized by a variety of techniques such as rapid solidification from the liquid state, mechanical alloying, plasma processing and vapor deposition (cf. [17]). Yet the requirements on the microstructure necessary for the

soft magnetic properties rule out quite a number of the available processes. Thus, controlled crystallization from the amorphous state seems to be the only method presently available to synthesize nanocrystalline alloys with attractive soft magnetic properties.

A typical nanocrystalline structure with good soft magnetic properties occurs if the amorphous state is crystallized by the primary crystallization of bcc Fe, before intermetallic phases like Fe-B compounds may be formed. Both an extremely high nucleation rate and slow growth of the crystalline precipitates are needed in order to obtain a nanoscaled microstructure. Such crystallization characteristics seems to be rather the exception than the rule and can be only obtained with appropriate alloy design. Thus, crystallization of conventional metallic glasses optimized for soft magnetic applications usually yields a relatively coarse grained microstructure of several crystalline phases with grain sizes of about 0.1-1 µm and, correspondingly, deteriorates the soft magnetic properties.

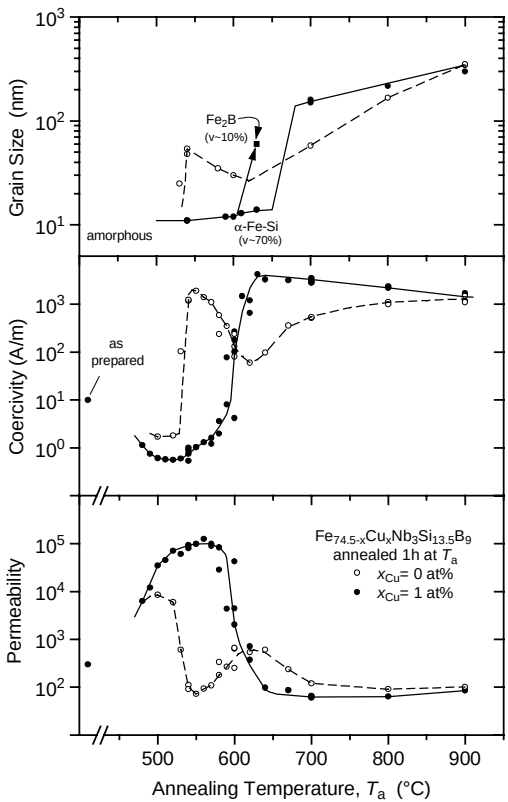

Figure 4. Average grain size, coercivity and initial permeability of $Fe_{74.5-x}Cu_xNb_3Si_{13.5}B_9$ (x = 0, 1 at%) as a function of the annealing temperature.

3.2.1 Fe-Cu-Nb-Si-B Alloys

The optimum alloy composition originally proposed [3] and subsequently not much changed is $Fe_{73.5}Cu_1Nb_3Si_{13.5}B_9$ (at%) and can be considered as a typical Fe-Si-B metallic glass composition with small additions of Cu and Nb (or other group IV to VI elements). The combined addition of Cu and Nb is essentially responsible for the formation of the particular nanocrystalline structure: copper enhances the nucleation of the bcc grains while niobium impedes coarsening and, at the same time, inhibits the formation of boride compounds.

Figure 4 summarizes the evolution of the microstructure and the soft magnetic properties with the annealing temperature. The nanocrystalline state is achieved by annealing at temperatures typically between about 500°C and 600°C which leads to primary crystallization of bcc Fe. The resulting microstructure is characterized by randomly oriented, ultrafine grains of bcc Fe-Si-20 at% with typical grain sizes

of 10–12 nm embedded in a residual amorphous matrix which occupies about 20-30% of the volume and separates the crystallites at a distance of about 1–2 nm (cf. [9]). These features are the basis for the excellent soft magnetic properties indicated by the high values of the initial permeability of about 10^5 and correspondingly low coercivities of less than 1 A/m. The magnetic properties and the underlying microstructure are rather insensitive to the precise annealing conditions within a wide range of annealing temperatures, T_a, of about $\Delta T_a \approx 50–100$°C. They develop in a relatively short period of time (about 10–15 min.) and do not much alter even after prolonged heat treatment of several hours. Only annealing at more elevated temperatures above about 600°C leads to the precipitation of small fractions of boride compounds like Fe_2B or Fe_3B with typical dimensions of 50 nm to 100 nm, while the ultrafine grain structure of bcc Fe-Si still persists. Further increase of the annealing temperature above about 700°C, finally yields grain coarsening. Both the formation of Fe-borides and grain coarsening deteriorates the soft magnetic properties significantly.

The annealing behavior of $Fe_{74.5}Nb_3Si_{13.5}B_9$, i.e. a similar alloy composition, but without Cu demonstrates the significance of the Cu-addition (Fig. 4). The crystallization of this Cu-free alloy is quite different and leads to a severe degradation of the soft magnetic properties compared to the original amorphous state. It, thus, resembles substantially that which is usually observed in conventional amorphous alloys. The average grain size upon the onset of crystallization is relatively large, up to about 60 nm with a broad scatter, and shows a distinct variation with the annealing temperature. Furthermore, annealing of the Cu-free alloy leads to the simultaneous or sequential formation of several crystalline phases.

The small grain size in the $Fe_{73.5}Cu_1Nb_3Si_{13.5}B_9$ alloy or similar alloy compositions is decisive for its soft magnetic behavior, but ultimately is only a prerequisite. The actual highlight of the nanocrystalline Fe-base alloys is that the phases formed on crystallization simultaneously can lead to low or vanishing saturation magnetostriction, λ_s. Figure 5 summarizes the situation in the Fe-Cu-Nb-Si-B system. It is the decrease of λ_s which is ultimately responsible for the simultaneous increase of the initial permeability upon nanocrystallization. Otherwise, the soft magnetic properties would be only comparable to that of stress-relieved amorphous Fe-based alloys.

While λ_s is fairly independent of the composition in the amorphous state it depends sensitively on the Si-content in the nanocrystalline state, passing through zero at low and at high Si concentrations around 16 at%. The composition dependence essentially reflects the compositional variation of λ_s found for polycrystalline α-$Fe_{100-x}Si_x$ (cf. [18]). The detailed behavior of λ_s can be understood from the balance of magnetostriction among the structural phases present in the nanocrystalline state, i.e. [19]

$$\lambda_s \approx v_{cr} \cdot \lambda_s^{FeSi} + (1 - v_{cr}) \cdot \lambda_s^{am}, \tag{4}$$

where λ_s^{FeSi} and λ_s^{am} denote the local magnetostriction constants of the α-Fe-Si grains and the residual amorphous matrix, respectively, and v_{cr} is the volume fraction of the crystalline phase.

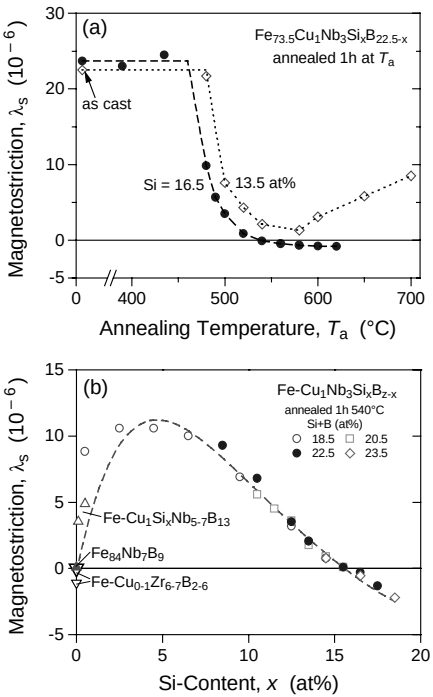

Figure 5. The saturation magnetostriction, λ_s, of Fe-Cu-Nb-Si-B alloys: (a) Influence of the annealing temperature, T_a and (b) influence of the Si-content in the nanocrystalline state. The figure includes the data for Fe-Nb-B (solid up triangle) and Fe-(Cu)-Zr-B alloys (open down triangles) from ref. [12].

Thus, near zero magnetostriction in nanocrystalline Fe-base alloys requires a large crystalline volume fraction with negative magnetostriction in order to compensate the high positive value of the amorphous Fe-based matrix. This is achieved either by a high Si-content in the bcc grains ($\lambda_s^{FeSi} \approx -6\times10^{-6}$ for α-$Fe_{80}Si_{20}$), as in the Fe-Cu-Nb-Si-B system, or if the grains consist of pure α-Fe ($\lambda_s^{Fe} \approx -4\times10^{-6}$) as in Fe-Zr-B alloys [12].

An important point to stress is that the superposition of the local magnetostriction constants to zero really results in stress-insensitivity of the magnetic properties as in amorphous Co(Fe)-base alloys. This is again a consequence of the smoothing effect of the exchange interaction for structural correlation lengths much smaller than the domain wall width. Thus, the nano-scale fluctuations in magneto-elastic anisotropy associated with the locally varying magnetostrictions are randomly averaged out which results in a single isotropic magnetostriction coefficient. The situation, thus, contrasts with that for large grained crystalline systems, where an average zero saturation magnetostriction does generally not imply stress-insensitivity of the hysteresis loop. Thus, the small grain size is also a decisive factor for the magnetostriction: although it does not directly influence the value of λ_s, it opens a *new* way to the achievement of isotropically low magnetostriction by combining the properties of different structural phases with the help of exchange interaction.

3.2.2 Further Alloy Compositions

The most superior soft magnetic properties are found for the original compositions around $Fe_{\sim74}Cu_1Nb_3Si_{13\text{-}16}B_{6\text{-}9}$ and are comparable to the excellent properties known so far from permalloys or Co-base amorphous alloys. The advantages, however, are the higher saturation induction of 1.2-1.3 T (twice the value of comparable near zero-magnetostrictive Co base amorphous alloys) and a significantly better thermal stability of the soft magnetic properties.

Yet a major driving force in the search for further alloy compositions was to increase the saturation magnetization towards the value of pure α -iron. The major hindrance towards such high iron content alloys results from by the requirement of a good glass forming ability. Thus, for the sake of a good glass forming ability, the Si-content in the Fe-Cu-Nb-Si-B-alloys cannot be simply reduced without substituting other glass formers for it. Such elements which extend the glass forming range at low Si and B-contents are group IVa to VIa transition metals [20]. The glass forming range is the widest for Hf containing alloys and decreases in the order of Zr>Nb≈Ta>Mo≈W>V>Cr. The most stable amorphous phase is, thus, obtained in alloys containing refractory metals with large atoms and low *d*-electron concentrations, i.e. particularly Zr, Hf, Nb and Ta.

In this way a second family of near-zero magnetostrictive, nanocrystalline alloys has been established which is based on $Fe_{\sim 84\text{-}91}(Cu_1)$-$(Zr,Nb)_{\sim 7}B_{2\text{-}9}$ and exhibits a still higher saturation magnetization up to 1.7 Tesla [12]. Although the outstanding soft magnetic properties of the original alloy system could not be reached up to now, the soft magnetic properties are better than those of amorphous Fe-base alloys or comparable to those of crystalline 50-60% Ni-Fe but combined with low magnetostriction and lower losses. These alloys and derivatives are currently still under intensive research. Their major draw-back is a lower glass forming ability and/or castability due to the oxygen reactivity of the Zr addition. Thus, these alloys presently are still restricted to the laboratory scale, since they require a far more sophisticated production technology than the more conventional Fe-Si-B compositions.

Interestingly, as a kind of precursor, the first example for soft magnetic behavior in the nanocrystalline state was given by O´Handley [21] for a devitrified glassy *cobalt* base alloy. However, the soft magnetic properties were inferior to the amorphous state and, thus, not very attractive, which to the present seems to be typical for cobalt based nanocrystalline materials. Indeed, the most promising properties so far have been found in *iron* based alloys.

It should be finally mentioned that the spectrum of accessible nanocrystalline systems can still be considerably expanded by thin film sputtering techniques. One example are Hf carbide dispersed nanocrystalline Fe-Hf-C films crystallized from the amorphous state [22]. They combine good thermal stability, good high frequency properties in the MHz range with low magnetostriction and high saturation induction of J_s =1.7 T which can be even increased up to 2.0 T by multilayering these films with Fe. Another example are (Fe,Co,Ni)-(Si,B)-(F,O,N) granular alloy films (cf. [22]) which at a saturation induction of about 1 T possess a uniquely high electrical resistivity of 10^3-10^4 μΩcm which makes them a possible candidate for future high-frequency devices.

4 Field Induced Anisotropies or Tailoring the Hysteresis Loop

Tailoring the hysteresis loop of a ferromagnetic material involves controlling the magnetic anisotropies, i.e. to avoid disturbative contributions e.g. from magneto-elastic interactions and to introduce small uniaxial anisotropies of well defined orientation and magnitude (cf. [24]). The latter is preferably realized by magnetic field annealing which induces a uniaxial anisotropy with an easy axis parallel to the direction of the magnetic

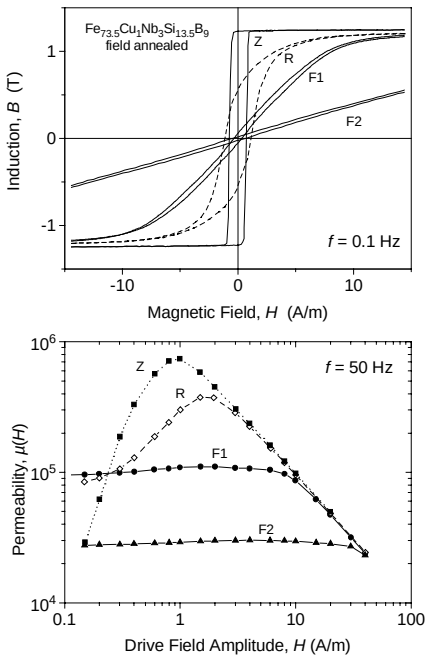

Figure 6. Typical dc-hysteresis loops and 50 Hz permeability after various forms of field annealing. The material shown is nanocrystalline $Fe_{73.5}Cu_1Nb_3Si_{13.5}B_9$ annealed for 1h at 540°C without (R) and with a magnetic field applied parallel (Z) and transverse (F2; $K_u \approx 20$ J/m^3, $\mu \approx 30\times10^3$) to the magnetic path. Sample F1 ($K_u \approx 6$ J/m^3, $\mu \approx 100\times10^3$) was first crystallized at 540°C and subsequently transverse field annealed at 350°C.

field applied during the heat treatment. Figure 6 shows typical examples of the hysteresis loop and the impedance permeability for a nanocrystalline $Fe_{73.5}Cu_1Nb_3Si_{13.5}B_9$ alloy as obtained after various heat treatments with and without magnetic field. The characteristic features of the specific example shown in Fig. 6 are the same for other nanocrystalline or amorphous materials.

Thus, almost perfect rectangular or flat shaped hysteresis loops can be obtained after field annealing which indicates that the field induced anisotropy clearly dominates over the residual contributions from magnetocrystalline and magneto-elastic anisotropies. Still, the induced anisotropy constant, K_u, can be tailored small enough in order to achieve highest permeabilities (for example, $K_u \approx 6$ J/m^3 and $\mu \approx 100\,000$ as for the F1-loop shown in Fig. 6).

The *flat shaped* loops (F1, F2) are obtained by transverse field annealing, i.e. by inducing a uniaxial anisotropy perpendicular to the ribbon axis. The magnetization process is determined by rotation of the magnetization vectors from the easy direction towards the ribbon axis. This results in a permeability, μ, practically constant up to ferromagnetic saturation which by

$$\mu = J_s^2/(2\,\mu_0\,K_u) \tag{5}$$

is directly related to the induced anisotropy energy constant, K_u.

The *rectangular* loop (Z) results after longitudinal field annealing. The uniaxial anisotropy is parallel to the ribbon axis and, thus, the magnetization process is dominated by 180° domain wall displacements. Highest maximum permeabilities can be achieved in this way. Since the domain wall energy is proportional to the square root of K_u , low induced anisotropies in this case facilitate domain refinement which results in good dynamic properties like e.g. reduced anomalous eddy current losses.

The *round* loop (R) results after conventional annealing without magnetic field. The magnetization process is a mixture of magnetization rotation and domain wall displacements. The characteristic features of the round loop are a remanence to saturation around 50%, a high initial and a high maximum permeability. Annealing without field,

however, does not necessarily mean that there are no induced anisotropies. As long as the annealing temperature is lower than the Curie temperature, there are always induced anisotropies along the direction of the local spontaneous magnetization within a ferromagnetic domain. The presence of a magnetic field just aligns the domains parallel and, thus, induces a uniform anisotropy. Thus, the heat treatment without a field produces a random distribution of uniaxial anisotropies induced parallel to the magnetization vector in each domain. In order to optimize the soft magnetic properties of the round loop it is again necessary to minimize the locally induced anisotropies which is preferably done by annealing above the Curie temperature, T_c, followed by rapid cooling.

The tremendous practical impact of field induced anisotropies is almost self-evident. Their understanding is the key for the reproducible control of the soft magnetic properties according to the demands of various applications. Actually, this does not only hold for the magnetic properties achieved after annealing but also for their thermal stability at application temperatures. Thus, the mechanisms of thermal aging, in principle, are the same as those which are used to tailor the magnetic properties during annealing but at a reduced kinetics due to the comparably lower operation temperature. Good thermal stability of the magnetic properties, therefore, also requires a possibly high activation energy and slow kinetics of anisotropy formation.

The induction of a magnetic anisotropy along the axis of the spontaneous magnetization is related to directional atomic pair ordering along this axis which minimizes spin-orbit coupling energy; the magnitude of K_u generally depends upon the alloy composition and the annealing conditions (cf. [25]).

4.1 AMORPHOUS ALLOYS

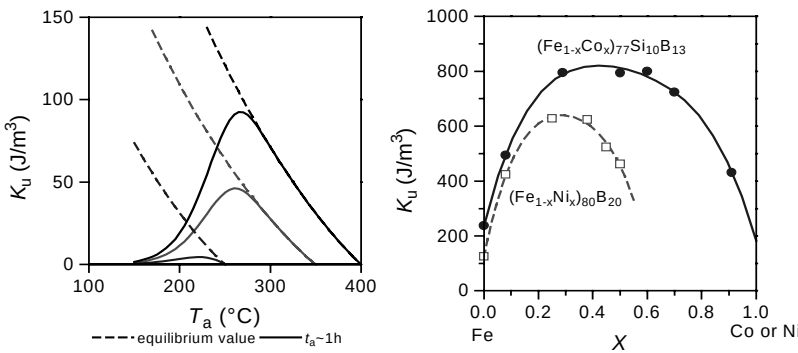

Figure 7. Dependence of the field induced anisotropy, K_u, in amorphous alloys on the annealing temperature, T_a, and the composition. The K_u vs. T_a curves on the left are a sketch of the typical behavior in near-zero magnetostrictive Co-base alloys with different Curie temperatures (after [24]). The figure on the right shows the equilibrium K_u of Fe-Ni-base and Fe-Co-base alloys annealed at 225°C and 300°C, respectively (after [25]).

Figure 7 shows the characteristic features of field induced anisotropies in amorphous metals which can be summarized as follows [24, 25]:

1. An anisotropy is only formed by annealing below the Curie temperature T_c, i.e. the driving force are magnetic interactions. The equilibrium value of K_u achieved after infinite time of annealing approximately scales with the square of the saturation magnetization at the given annealing temperature.

2. The anisotropy formation is governed by thermal activation. At lower annealing temperatures the kinetics are too slow to reach the equilibrium value which results in the typical maximum of K_u at a certain annealing temperature.

3. Alloys with two or more different kinds of magnetic metallic elements show considerably stronger field induced anisotropies than amorphous alloys with only one transition element.

Principally any level of K_u can be adjusted by appropriate choice of the annealing temperature and time. The annealing conditions which can be realized in practice, however, only allow a K_u variation of a about a factor 3–5 around the maximum in the K_u vs. T_a curve in Fig. 7. The latter is dictated by the alloy composition. Accordingly, low values of K_u, i.e. high permeabilities, can be only achieved in alloys with preferably only one magnetic transition metal and a possibly low Curie temperature. which at the same time means a low saturation magnetization (cf. Fig. 3).

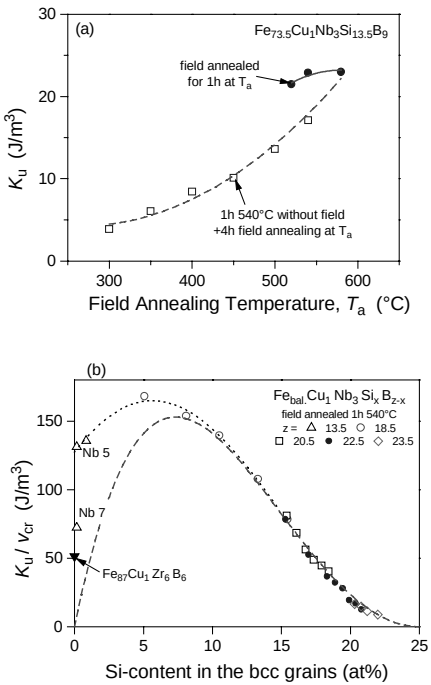

Figure 8. Field induced anisotropy, K_u, in nanocrystalline Fe-Cu-Nb-Si-B alloys: (a) Influence of the annealing conditions and (b) role of the composition in the nanocrystalline state for the equilibrium K_u .

4.2 NANOCRYSTALLINE ALLOYS

The principal features of anisotropy formation in nanocrystalline alloys [26, 27] are similar to the amorphous case and are summarized in Fig. 8.

If the material is nanocrystallized first without applied field and subsequently field annealed at lower temperatures, the resulting K_u depends on the annealing temperature, T_a, and time, t_a and behaves similar to the amorphous case. However, the kinetics is considerably slower [26] which shifts the maximum of the K_u vs. T_a curve to considerably higher annealing temperatures. This allows to tailor lowest induced anisotropies, i.e. highest permeabilities but with a significantly better thermal stability than in amorphous alloys or even in permalloys.

If the field annealing is performed during nanocrystallization, the induced anisotropy reaches a maximum value

which is relatively insensitive to the precise annealing conditions and, thus, corresponds to the equilibrium value characteristic for the alloy composition [27].

The Curie temperature of the bcc grains ranges from about T_c =600°C to 750°C (depending on composition) and is considerably higher than the T_c of the amorphous matrix (200°C to 400°C). Thus, the anisotropy induced by a magnetic field applied during nanocrystallization at 540°C primarily originates from the bcc grains [27]. Accordingly, the induced anisotropy in nanocrystalline Fe-Cu-Nb-Si-B-alloys is mainly determined by the Si-content and the fraction, v_{cr}, of the bcc grains. The dependence of K_u/v_{cr} on the Si-content in the bcc grains (Fig. 8b) is comparable with that observed for conventional α-FeSi single crystals [28] where the formation of the field induced anisotropy has been proposed to arise from the directional ordering of Si-atom pairs.

The decrease of K_u with increasing Si content, in terms of Néel´s [29] theory, can be related to the formation of a DO_3 superlattice structure for Si-concentrations above about 10 at%: For completely ordered Fe_3Si, the lattice sites for the Fe and Si atoms are entirely determined by chemical interactions, allowing no degree of freedom for an orientational order. However, for a composition $Fe_{1-y}Si_y$ with less than 25 at% Si no complete DO_3 order can be reached and Fe atoms will occupy the vacant sites in the Si sublattice. The way the latter is done provides the necessary degrees of freedom for an orientational order. Thus, the present anisotropy data above about 10 at% Si can be well described by (see dashed line in Fig. 8b) [30]

$$K_u / v_{cr} = K_o \, c^2 \, (1 - c^2) \,, \tag{6}$$

where $c = (1 - 4\,y)$ denotes the fractional concentration of Fe at Si sites. The low K_u-level due to the superlattice structure at higher Si-contents is an additional key factor for the high initial permeabilities which can be achieved in these alloys despite their high Curie temperature and their high saturation induction.

5 Application Oriented Properties

Low effective magnetocrystalline anisotropy and low or vanishing magnetostriction are the key to superior soft magnetic properties. There are only a few alloy compositions that exhibit this combination of properties: the permalloys, Sendust, manganese-zinc ferrites, the amorphous cobalt-based alloys and, the nanocrystalline iron-based alloys.

Of course, soft magnetic applications not only require superior soft magnetic properties in terms of highest permeability and lowest coercivity. A well defined shape of the hysteresis loop with not necessarily highest but a well defined level of permeability is as important. This is generally realized by magnetic field annealing. In particular the flat type hysteresis loops have been proven to be particularly useful for many applications.

High saturation induction, low losses, good high frequency behavior, favorable temperature dependence and high thermal stability of the soft magnetic properties are further requirements for most applications.

5.1 SATURATION INDUCTION AND PERMEABILITY

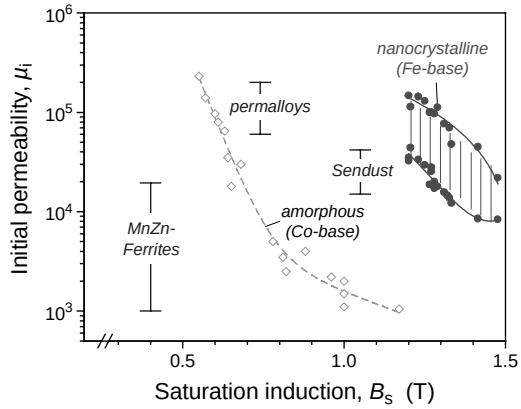

Figure 9. Typical initial permeabilities and saturation inductions for low magnetostrictive, soft magnetic materials.

Figure 9 compares the magnetic properties of flat type near-zero magnetostrictive alloys. The clear advantage of nanocrystalline alloys is that they combine the highest achievable permeabilities (up to $\mu_i \approx 300\times10^3$) and the simultaneously highest saturation induction of typically $B_s \approx 1.2$ - 1.3 T. The benefit of amorphous materials is that they allow a much wider range of property variation. Thus, the initial permeability of near-zero magnetostrictive alloys can be varied continuously by more than two orders of magnitude from about $\mu_i \approx 1\times10^3$ up to $\mu_i \approx 300\times10^3$.

5.2 LOSSES

Both amorphous and nanocrystalline alloys generally reveal low losses and a high permeability even at elevated frequencies up to several 100 kHz (cf. [3, 10]). Fig. 10 gives a comparative example for the core losses. The favorable high frequency behavior, comparable or even better than in Mn-Zn ferrites, is essentially related (1) to the thin ribbon gauge of $d \approx 20$ µm inherent to the production technique and (2) to a relatively high electrical resistivity of typically $\rho \approx$ 100-130 µΩcm. Both reduce eddy current losses. In particular, low remanence ratio materials show the best dynamic properties due to the homogeneous change of magnetization by rotation which avoids *anomalous* eddy current losses. Lowest losses are hereby found in near zero-magnetostrictive alloys due to (1) their low coercivity which minimizes the hysteresis losses and due to (2) the absence of magneto-elastic resonances which in magnetostrictive alloys can produce very significant excess losses.

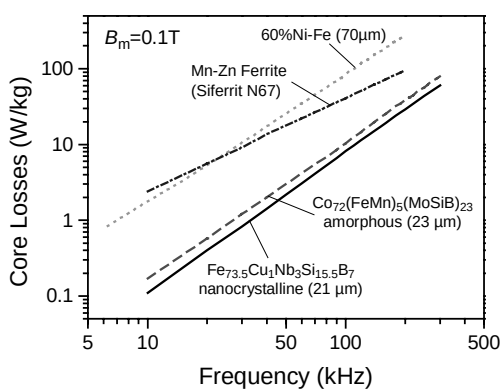

Figure 10. Core losses vs. frequency for low remanence, soft magnetic materials used for high frequency power transformers.

5.3 TEMPERATURE DEPENDENCE OF THE MAGNETIC PROPERTIES

Figure 11 shows the temperature dependence of the permeability. In highly permeable crystalline alloys, like permalloy (80%NiFe), the magnetocrystalline anisotropy constant K_1 is adjusted to zero by alloying and annealing which, however, is effective only for a certain temperature. Thus, the temperature dependence of K_1 yields a pronounced variation of the soft magnetic properties around the temperature where K_1 is zero (cf. [31]). In particular, the drop of permeability towards lower temperatures (because of $K_1>0$) can be a problem for certain applications like magnetic cores for ground fault interrupters. In comparison, in nanocrystalline and amorphous materials the magnetocrystalline anisotropy is averaged out by exchange interaction which is effective over a large temperature range. Accordingly the magnetic properties vary smoothly in both materials. In amorphous alloys the behavior is mainly determined by induced anisotropies whose magnitude decreases and, thus, the permeability typically increases with increasing temperature. The situation is somewhat more complex in nanocrystalline materials, since the intergranular exchange coupling is reduced when approaching the Curie temperature of the amorphous matrix [7]. At application temperatures, this mechanism typically causes a smooth decrease of permeability with increasing temperature [32]. This decrease, however, can be compensated by appropriate field annealing. Thus, as exemplified in Fig. 11, it is possible to adjust an almost negligible temperature variation of μ over the whole range of application temperatures.

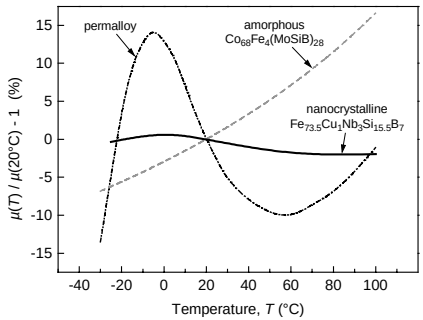

Figure 11. Relative change of the initial permeability normalized to its room temperature value vs. the typical range of application temperatures for comparable, highly permeable soft magnetic materials.

Figure 12, finally, compares the temperature dependence of the magnetization and magnetostriction of an amorphous Co-base alloy and a nanocrystalline alloy. In both cases λ_s passes through zero near room temperature. The temperature variation around $\lambda_s=0$, however, is more pronounced for the nanocrystalline alloy. Still, the magnetostriction of the nanocrystalline alloy can be kept as small as $|\lambda_s|<0.2\times10^{-6}$ for typical application temperatures.

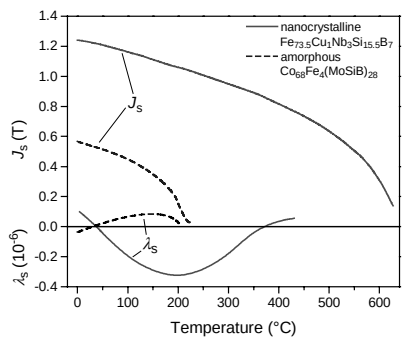

Figure 12. Temperature dependence of the saturation magnetization, J_s, and the saturation magnetostriction, λ_s, of nanocrystalline $Fe_{73.5}Cu_1Nb_3Si_{15.5}B_7$ (full lines) and a comparable, highly permeable amorphous Co-base alloy (dashed lines).

5.4 THERMAL STABILITY

Still the major requirement at elevated application temperatures is the long-term thermal stability of the magnetic properties. Empirically, thermally induced aging of the magnetic properties is the more critical the better these properties are. Apart from temperature and time, the aging behavior also depends on the magnetizing conditions during operation whose limiting cases are the remanent (or demagnetized) state and the ferromagnetically saturated state, respectively. The latter generally represents the worst case. Figure 13 compares the aging behavior of a highly permeable amorphous Co-base alloy, nanocrystalline $Fe_{73.5}Cu_1Nb_3Si_{15.5}B_7$ and crystalline Ni-Fe. Thus, thermal aging is a particular problem for highly permeable Co-base alloys and limits the upper continuos service temperature to about 80° - 100°C. In comparison, the thermal stability of the nanocrystalline material surpasses by far that of amorphous alloys and even that of permalloys which allows higher continuous service temperatures up to 150°C.

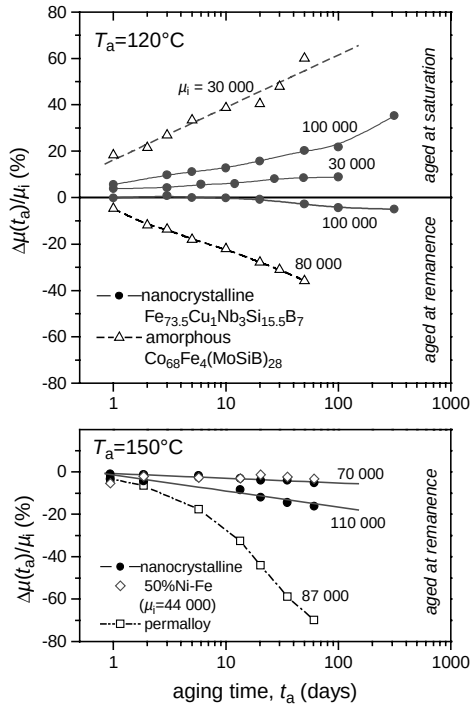

Figure 13. Relative change of the initial permeability vs. the time of thermal aging at elevated application temperatures. The comparison is made for highly permeable materials with low remanence hysteresis loops.

The excellent thermal stability of the magnetic properties is a further highlight of soft magnetic nanocrystalline alloys and is closely related to the factors governing the anisotropy formation discussed before. Thus, the reduced degrees of freedom for anisotropy formation due to the superlattice structure together with the high Curie temperature allows one to stabilize very small induced anisotropies and, hence, high permeabilities at annealing temperatures much higher than possible for highly permeable amorphous alloys or permalloy. This essentially reduces the kinetics for anisotropy changes at application temperatures. In comparison with amorphous metals, the thermal stability is additionally improved by the more stable crystalline structure.

6 Conclusions

In summary, the best static and dynamic soft magnetic properties are presently achieved as well in amorphous Co-base as in nanocrystalline Fe-base alloys. Both alloy systems reveal isotropic near-zero magnetostriction. Apart from its higher saturation induction, however, the nanocrystalline material moreover shows a much better thermal stability of its magnetic properties than its amorphous counterpart. Additionally, it is based on the inexpensive raw materials iron and silicon. Accordingly, nanocrystalline alloys provide an invaluable supplement to the existing soft magnetic materials manifested in a steadily increasing number of applications. Yet, the variability of their soft magnetic properties as well as their form of delivery so far is still restricted compared to amorphous or other soft magnetic materials. Thus, amorphous alloys may reveal good soft magnetic properties already in the as quenched state or after moderate annealing. They can be delivered as a semi-finished, ductile product useful for e.g. flexible magnetic screening or for sensor applications, most noticeably in electronic article surveillance. Accordingly, the major draw-back of the nanocrystalline materials is the severe embrittlement upon crystallization which requires final shape annealing and restricts their application mainly to toroidally wound cores. Yet, the situation is similar for highly permeable amorphous alloys due to the necessary stress relief treatment which also causes embrittlement.

The key to the properties of both amorphous and nanocrystalline soft magnetic alloys is that the structural correlation length is much smaller than the ferromagnetic correlation length. Thus, the magneto-crystalline anisotropy is randomly averaged out by exchange interaction. Still, in nanocrystalline systems this averaging effect of exchange interaction in the small grain size regime allows one to combine the individual properties of different structural phases which expands the variability of property tailoring over that of alloying single phases. The isotropically low or vanishing magnetostriction which can be achieved in this new way is a particular example.

7 References

1. Cahn, R.W. (1993) Background to rapid solidification processing, in H.H. Liebermann (ed.), *Rapidly Solidified Alloys*, Marcel Dekker, Inc., New York, Basel, Hong Kong, pp. 1-15.
2. Boll, R., Hilzinger, H.R. and Warlimont, H. (1983), Magnetic material properties and applications of metallic glasses, in R. Hasegawa (ed), *The Magnetic, Chemical and Structural Properties of Glassy Metallic Alloys*, CRC Press, pp. 183-201
3. Yoshizawa, Y, Oguma, S. and Yamauchi, K. (1988), New Fe-based soft magnetic alloys composed of ultrafine grain structure, *J. Appl. Phys.* **64**, 6044-6046
4. Pfeifer, F. and Radeloff, C. (1980) Soft magnetic Ni-Fe and Co-Fe alloys, *J. Magn. Magn. Mat.* **19**, 190-207
5. Luborsky, F. E. (1961) High coercive materials, *J. Appl. Phys.* **32**, 171S-183S
6. Manaf, A., Buckley, R.A. and Davies, H.A. (1993), New nanocrystalline high-remanence Nd-Fe-B alloys by rapid solidification, *J. Magn. Magn. Mat.* **128**, 302-306
7. Herzer, G. (1989) Grain structure and magnetism of nanocrystalline ferromagnets, *IEEE Trans.Magn.* **25**, 3327-3329
8. Herzer, G. (1990) Grain size dependence of coercivity and permeability in nanocrystalline ferromagnets, *IEEE Trans.Magn.* **26**, 1397-1402
9. Herzer, G. (1995), Nanocrystalline soft magnetic materials, *Physica Scripta* **T49**, 307-314 and references therein
10. Boll, R. (1990) *Weichmagnetische Werkstoffe*, Vacuumschmelze GmbH, Siemens AG Verlag, Berlin

11. Vacuumschmelze GmbH (1993) Toroidal Cores of VITROPERM, data sheet PW-014
12. Suzuki, K., Makino, A., Kataoka, N., Inoue A. and Masumoto, T. (1991), Soft magnetic properties of nano-
crystalline bcc Fe-Zr-B and Fe-M-B-Cu alloys with high saturation, *J. Appl. Phys.* **70**, 6232-6237
13. Alben, R., Becker, J. J. and Chi, M. C. (1978) Random anisotropy in amorphous magnets, *J. Appl. Phys.* **49**, 1653-1658
14. O'Handley, R.C.(1987) Physics of ferromagnetic amorphous alloys, *J. Appl. Phys.* **62**, R15-R59
15. Fujimori, H., Kikuchi, M., Obi, Y. and Masumoto T. (1976) New Co-Fe amorphous alloys as soft magnetic materials, *Sci. Rep. Res. Inst. Tohoku Univ. Ser. A*, **26**, 36
16. Hilzinger, H.R. and Kunz, W. (1980) *Magnetic properties of amorphous alloys with low magnetostriction*, J. Magn. Magn. Mat., 15-18, 1357
17. Suryanarayana, C. (1995) Nanocrystalline materials, *International Materials Reviews*, **40**, 41-64
18. Yamamoto, T. (1980) *The Development of Sendust and Other Ferromagnetic Alloys*, Komiyama Printing, Chiba, Japan
19. Herzer, G. (1991) Magnetization process in nanocrystalline ferromagnets, *Mat. Sci. and Eng.* **A133**, 1-5
20. Inoue A., Kobayashi, K., Kaneira J. and Masumoto, T. (1981) *Sci. Rep. Res. Inst. Tohoku Univ.* A **29**, 331
21. O'Handley, R. C., Megusar, J., Sun, S.-W. Hara and Y. Grant, N.J. (1985), Magnetization process in devitrified glassy alloy, *J. Appl. Phys.* **57**, 3563-3565
22. Hasegawa, N., Saito, M., Kataoka, N. and H. Fujimori (1993), Soft magnetic properties of carbide-dispersed nanocrystalline films with high thermal stability, *J. Mater. Eng. and Perform.* **2,** 181-192
23. Fujimori, H. (1995), Structure and 100MHz soft magnetic properties in multilayers and granular thin films, *Scripta Metallurgica et Materialia* **33**, 1625-1636
24. Hilzinger, H.R. (1980) Amorphe Magnetwerkstoffe, *NTG-Fachberichte* **76**, VDE Verlag, pp. 283-306
25. Fujimori, H. (1983), Magnetic Anisotropy, in F.E. Luborsky *(ed), Amorphous Metallic Alloys*, Butterworths, London, pp.300-316 and references therein
26. Yoshizawa, Y. and Yamauchi, K. (1990), Induced magnetic anisotropy and thickness dependence of magnetic properties in nanocrystalline alloy "Finemet", *IEEE Translation J. On Magnetics* **5,** 1070-1076
27. Herzer, G. (1994), Magnetic field induced anisotropies in nanocrystalline Fe-Cu-Nb-Si-B alloys, *Mat. Sci. and Eng.* **A181**/**A182** , 876-879
28. Sixtus, K. (1969), Anisotropie in Eisen-Silizium-Einkristallen nach Glühen im Magnetfeld, *Z. angew. Physik* **28**, 270-274
29. Néel, L. (1954), Anisotropie magnétique superficielle et substructures d'orientation, *J. Phys. Radium* **15**, 225-239
30. Herzer, G. (1995), Magnetostriction and induced anisotropies in naocrystalline Fe-Cu-Nb-Si-B alloys, in M. Vazquez and A. Hernando (eds.), *Nanostructured and Non-Crystalline Materials*, World Scientific Publishing, Singapore, pp. 449-460
31. Pfeifer, F (1992), Nickel-iron alloys, in J. Evetts (ed.), *Concise Encyclopedia of Magnetic & Superconducting Materials*, Pergamon Press, Oxford, pp. 349-356
32. Yoshizawa, Y. and Yamauchi, K. (1991), Magnetic properties of nanocrystaline Fe-based soft magnetic alloys, *Mat. Res. Soc. Symp. Proc*. **232**, 183-195